MNRAS **000**, 000–000 (0000) Preprint 6th April 2022 Compiled using MNRAS LATEX style file v3.0

Breaking Down the Role of Ionization and Recombination During Common Envelope Evolution I. Methods and Initial Results

Luke Chamandy,[1]★ et al.
[1]*Department of Physics and Astronomy, University of Rochester, Rochester NY 14627, USA*

6th April 2022

ABSTRACT

We perform simulations to study recombination and ionization during common envelope (CE) evolution, and develope techniques to track the various ionic transitions in space and time. Our simulations involve a 2 $M_\odot$ red giant branch primary and a 1 $M_\odot$ point particle secondary: one run employs a realistic tabular equation of state (EOS) that accounts for ionization and recombination and another employs an ideal gas EOS. By the end of each simulation ($>$ 100 orbits, $>$ 100 d), the mutual orbital energy of the core particles decreases at a near-constant rate and in both cases extrapolation to late times suggests a CE timescale of (1–10) yr. During the first half of the simulations the unbound mass is 10–20 per cent larger in the tabular EOS run and the particle orbital energies are virtually the same in the two runs, implying that released recombination energy helps to unbind the envelope. Most of this recombination energy is released by helium and hydrogen but at later times we find that recombination of metals may be important. By simulation end, the orbital separation is slightly larger in the tabular EOS run, apparently because released recombination energy expands the envelope, reducing drag. Consequently, there is extra energy transfer from particles to envelope in the ideal gas run, which partially compensates for the lack of recombination energy. Unfortunately, from about the halfway point, artificial transfer of energy from the ambient medium to bound envelope gas starts to become significant and may contribute to envelope unbinding; we discuss how this limitation could be overcome in future work.

Key words: binaries: close – stars: AGB and post-AGB – stars: kinematics and dynamics – stars: mass loss – stars: winds, outflows – hydrodynamics

1 INTRODUCTION

In the common envelope (CE) scenario, typically a giant star engulfs a much smaller companion and the companion and core of the giant spiral in together until either the envelope is ejected or the core and companion merge (Paczynski 1976). The CE phase is shortlived and hence hard to observe. However, understanding CE evolution (CEE) is crucial for understanding phenomena as wide-ranging as neutron star-neutron star mergers, supernovae type Ia and planetary nebulae (for a recent review see Ivanova et al. 2020). While theoretical work on CEE has come a long way, simulating CEE up to a realistic end state (e.g. complete envelope ejection and stabilization of the orbit) has still not fully been achieved. The overarching reason for this is that simulating such a large dynamic range of spatial and temporal scales remains very challenging.

Nevertheless, such calculations have been useful in constraining the effects of various physical processes during CEE. One such process is the recombination of ions and electrons as the envelope expands and cools, which releases recombination energy. As has become somewhat standard in the CE literature, we define recombination energy as the *latent* energy contained by a plasma that would be released upon recombination. After this energy is released, it may help to unbind the envelope, but it does not have any effect before the ions and electrons recombine.

While the recombination energy content of the intial envelope is generally substantial and thus could potentially play an important role in envelope unbinding, its efficacy remains somewhat unclear. This is partly because some released recombination energy radiates away (Soker & Harpaz 2003; Ivanova et al. 2013; Sabach et al. 2017; Ivanova 2018; Grichener et al. 2018; Soker et al. 2018; Reichardt et al. 2020; Lau et al. 2022). The question of how much is radiated is not addressed in the present work. Rather, we ask: what difference does recombination energy make to CEE, assuming (optimistically) that released recombination energy is thermalized locally? In particular, at any given time, how much extra envelope mass is unbound owing to this effect, where in the envelope does this extra unbinding happen, and what are the relative contributions of the various ionic species? Even in this optimistic case that ignores radiation, some recombination energy would be released in already unbound gas, and would thus play little to no role in envelope unbinding. Clearly, there is an efficiency associated with the transfer of released recombination energy to binding energy of the remaining envelope.

★ lchamandy@pas.rochester.edu

Sometimes authors count gas as unbound if its total energy density, including that of the recombination energy, is positive. This is misleading because it greatly overestimates the role of recombination energy in envelope unbinding. First, this energy is still latent. Second, when it eventually gets released it might not contribute much to unbinding owing to the inefficiencies mentioned above. A more reasonable approach is to include only kinetic(including perhaps thermal) and potential energies in assessing whether material is unbound, and compare the unbound mass in a simulation with a realistic tabular EOS that includes recombination energy with a simulation that does not. If cooling is neglected, it is appropriate to use a $\gamma = 5/3$ ideal gas EOS for the latter simulation. When such a comparison has been made (Ohlmann 2016; Reichardt et al. 2020; Sand et al. 2020; Lau et al. 2022), it has been found that the unbound envelope mass is significantly higher in the tabular EOS run. Moreover, the fractional difference in the unbound mass curves between the runs usually increases with time, indicating that the effect becomes more important at late times.[1]

While it is perhaps generally agreed that recombination energy often helps envelope unbinding, the details are still emerging. Reichardt et al. (2020) was the first to include a spatial analysis of where recombination of the various species is happening during a CE simulation. They then compared this data with data of where unbinding is happening in both $\gamma = 5/3$ and tabular EOS runs, allowing them to infer how recombination affects unbinding. In this work we take a somewhat different and complementary approach by employing tracers to track gas of a given ionization species at $t = 0$. By comparing maps of these tracers at a given time t with maps of the ionization state, it becomes possible to determine which gas has experienced net recombination or ionization, and how much energy this recombination (ionization) has released (absorbed).

The structure of the paper is as follows. In Section 2, we explain the methods used in the setup, running and analysis of the simulations. Then, in Section 3, we describe our physical model, including the initial conditions and the parameters of the runs performed. Results are then presented in Section 4. In Section 4.2 we present the evolution of the unbound mass with time, in Section **??** we analyze the transfer of energy between the various components, and in Section 4.3 we explore in detail the ionic evolution and the release of recombination energy. We discuss our results in Section 5 and conclude in Section 6. An assessment of the role of various numerical parameters is presented in Appendix A.

2 METHODS

Our study involves a binary system consisting of a red giant branch (RGB) primary star and a point particle (gravitation only) secondary representing a main sequence star or white dwarf. The initial density and pressure profiles of the primary are mapped to our 3D grid from a 1D Modules for Experiments in Stellar Astrophysics (MESA) snapshot (Paxton et al. 2011, 2013, 2015, 2019). The snapshot is taken from a MESA release 12778 simulation. It matches almost exactly the snapshot used for our previous RGB simulations using release 8845 (Chamandy et al. 2018, 2019b), except that this time we increased the spatial resolution by a factor of about 20 to make the profile smoother.

The pressure scale height near the core and at the stellar surface of the MESA profile are too small for a 3D simulation to resolve. Therefore, we cut out the RGB core and replaced it with a spline-softened gravitating point particle, with softening length $r_{\rm soft} = 2.41\,{\rm R}_\odot$, equal to the cut radius, along with a core density and pressure profile obtained by solving a modified Lane-Emden equation, which also incorporated an iteration to ensure that the mass below the cut radius is preserved (Ohlmann et al. 2017; Chamandy et al. 2018). The softening radius of the secondary is the same as that of the RGB core particle.

The ambient medium has uniform density $\rho_{\rm amb} = 1.0 \times 10^9\,{\rm g\,cm^{-3}}$ and uniform pressure $P_{\rm amb} = 1.0 \times 10^5\,{\rm dyn\,cm^{-2}}$. The value of $P_{\rm amb}$ is chosen such that by adding $P_{\rm amb}$ to the pressure everywhere, the RGB pressure profile effectively gets truncated just inside the outer radius of the star to avoid the small pressure scale height there. The value of $\rho_{\rm amb}$ is about 7 times smaller than the density at the outer radius of the star R_1; smaller values are possible but would result in a higher ambient temperature and prohibitively small timesteps. We find that we require at least eight resolution elements per scale height to adequately resolve the initial stellar profile. This number was determined by studying the smoothness and stability of both the core and surface, where the scale heights are smallest, during the first ~ 1 d of the simulations.[2]

We utilize the adaptive mesh refinement (AMR) code AstroBEAR (Cunningham et al. 2009; Carroll-Nellenback et al. 2013), and employ an HLLC Riemann solver. The simulation box of side length $1150\,{\rm R}_\odot$ is discretized into 512^3 AMR level 0 cells, corresponding to a base resolution of $\delta_0 \approx 2.25\,{\rm R}_\odot$. Initially, the envelope and some of the ambient medium surrounding the RGB star was resolved at AMR level 4, or $\delta_4 \approx 0.140\,{\rm R}_\odot$, and this refinement zone reduced in size gradually as the particle separation a reduced. However, unlike in our previous RGB simulations, AMR level 5, with $\delta_5 \approx 0.070\,{\rm R}_\odot$, was added around the point particles out to slightly farther than the softening sphere. This extra level of refinement helps to conserve energy and to avoid artificial reduction of the central density and pressure during the simulation. Buffer zones with 16 cells were included to smoothly transition between AMR levels. At $t = 25.2$ d, the softening radius around the particles was halved to $\approx 1.2\,{\rm R}_\odot$ and a sixth level of refinement was added, with $\delta_6 \approx 0.035\,{\rm R}_\odot$. At $t = 50.5$ d the softening radius was again halved to $\approx 0.6\,{\rm R}_\odot$ AMR level 7 was added, with $\delta_7 \approx 0.018\,{\rm R}_\odot$.

In Appendix A3 we track the change in the total energy of the simulation, and show that it does not exceed ??????% for any of the runs [Luke comments: angular momentum conservation], which gives us confidence that our numerical approach is reasonable.

2.1 Tracers

Tracers were added to track the core gas ($r_{\rm i} \leqslant r_{\rm soft}$), envelope ($r_{\rm soft} < r_{\rm i} \leqslant R_1$) and ambient ($r_{\rm i} > R_1$). Tracking the ambient material allows us to exclude it in postprocessing. Tracers were also added to track the initial hydrogen and helium ionization states of the gas. This way, by comparing the ionization state computed by the Saha equation with the original ionization state, one can deduce how the ionization state of the gas changes during the simulation. As the tracer density is equal to the total gas density where the

[1] For a more extensive review of the literature on the effects of ionization/recombination on CEE, we refer the reader to Reichardt et al. (2020).

[2] We did not perform a preliminary run to prepare the initial condition for the simulation. We found in the past that including such a relaxation run did not cause an important difference in the results, and our results have shown good quantitative agreement with similar simulations by other authors (Chamandy et al. 2019a). Moreover, we have found that artifacts due to the Cartesian grid can be magnified in such a preliminary run because the star is motionless.

tracer is located, tracers are not as useful for tracking ionic species from locations where they are not the dominant species, relative to other species of the same element. For this reason, we chose to place tracers for a given ionization state at locations where that ionization state was higher than others of the same element. Because the density of a given species depends exponentially on temperature, transitions in the dominant species are rather sharp, so this is not an important limitation. Because the mass fractions of all elements are constant within the envelope, as determined from MESA, one can simply multiply by the hydrogen mass fraction (0.69) or helium mass fraction (0.29) to obtain the approximate density of the tracer (e.g. gas that was originally HIII). Also, because the pressure very close to the stellar surface is replaced by the (larger) ambient pressure, the temperature at that location is higher than in the MESA snapshot. This causes gas at the surface to be ionized from $t = 0$, but the tracer is based on the MESA model.

2.2 Equation of State

Most of our simulations make use of the MESA tabular EoS, which has been adapted for use in AstroBEAR. However, we modified the MESA EoS by subtacting the radiation component of the specific energy aT^4/ρ, where T is temperature, ρ is gas density and a is the radiation constant. In the original MESA RGB profile, the ratio of this component to the local gas thermal specific energy $3k_{\rm B}T/(2\mu m_{\rm H})$, where $k_{\rm B}$ is the Boltzman constant and μ is the mean molecular mass units of the hydrogen mass $m_{\rm H}$, reaches a maximum of 20% at $r \approx 0.6\,{\rm R}_\odot$, but the ratio of the net energy contributions over the entire star is $< 0.1\%$. If included, the radiation energy leads to a high internal energy density in the high-temperature ambient medium, which could help to artificially unbind the envelope through mixing; hence we chose to exclude it. Moreover, this choice is consistent with the fact that radiation pressure is not included in the MESA EoS, though it is included in the stellar models computed in MESA. On the other hand, when preparing the simulation initial condition, we chose to make the gas pressure equal to the total pressure (gas plus radiation) in the MESA 1D RGB profile.

3 MODEL

3.1 Initial conditions

[Luke comments: Discuss MESA models and present a few plots] The profile extends to $R_1 = 48.1\,{\rm R}_\odot$. which is initialized at a separation $a_{\rm i} = 49\,{\rm R}_\odot$. Limits to computational resources prevent us from using a larger, more realistic, value of $a_{\rm i}$. The primary is not made to rotate initially.

[Luke comments: Mention similarity to Ohlmann+16,Prust+Chang19]

In any case, our main goal involves a comparison between runs which use the same initial conditions, we consider these various choices to be reasonable.

3.2 Physical parameters of the runs

[Luke comments: Summarize the various runs]

4 RESULTS

- Mention Fig. 2 and 3, top row (density) and second row (temperature)
- Summarize section

4.1 Orbital Evolution

- Mention Fig. 4
- Mention green curves in Fig. 5

- Contrast nearly constant rate of change of total particle energy with *apparent* assymptotic behaviour of separation → claims in the literature that the separation 'stalls' are misleading
- Use the alpha prescription (without recombination energy) along with extrapolation of the particle energy curve to predict how long it would take to reach the true final separation (alternatively could extrapolate separation curve but I am thinking extrapolating energy curve would be easier)
- Discussion of how such predictions will never be perfect because of the uncertainty in the the efficiency parameters, but also the arbitrariness of the definition for "unbound" material.
- Argue that certain claims in the literature that a particular simulation shows that the energy formalism is wrong are unfounded, because they

1) misrepresent the final separation in the simulation as the actual final separation even though it is still decreasing in the simulation,
2) choose an unrealistic definition for unbound mass (usually the ridiculous definition that includes latent recombination energy) and
3) the numerics likely makes the separation curve shallower than it should be (particularly when the separation decreases to below twice the initial softening radius)

4.2 Envelope energization and unbinding

- Mention Fig. 2 and 3, bottom two rows (unbound mass)
- Mention Fig. 6 for unbinding
- Mention Fig. 5, to argue that can only plot up to ~ 50 days because after that unbound mass rises but energy of bound gas does not reduce, so energy transfer from ambient could be contributing to unbinding.
- Mention Fig. 7, for solid blue curve, to argue that release of rec en causes extra unbinding
- Mention Fig. 5, to argue that release of rec en also causes expansion (also argue unbinding+expansion not due to difference in orbital energy release so must be due to recombination)
- Mention Fig. 7, comparing solid blue and green curve, to argue that extra orbital energy release in ideal gas run partially compensates for lack of recombination energy, in terms of contributing to energy budget of bound gas (and helping to unbind envelope)
- Estimate the value of $\alpha_{\rm rec}$ for the efficiency of using recombination energy (restrict to first 50 days)
- Mention that unbound mass curves are almost the same at late times for the two runs (but not reliable)
- Nevertheless, worth mentioning rate of unbinding at late times.
- Use this late unbinding rate along with particle energy curve to estimate value of $\alpha_{\rm CE}$ (very tentative)

4.3 Recombination and Ionization

- Provide a brief outline for this section

4.3.1 Release of recombination energy

- Mention Fig. 7 and discuss comparison between blue solid and blue dashed curves
- Argue that metals likely play a role

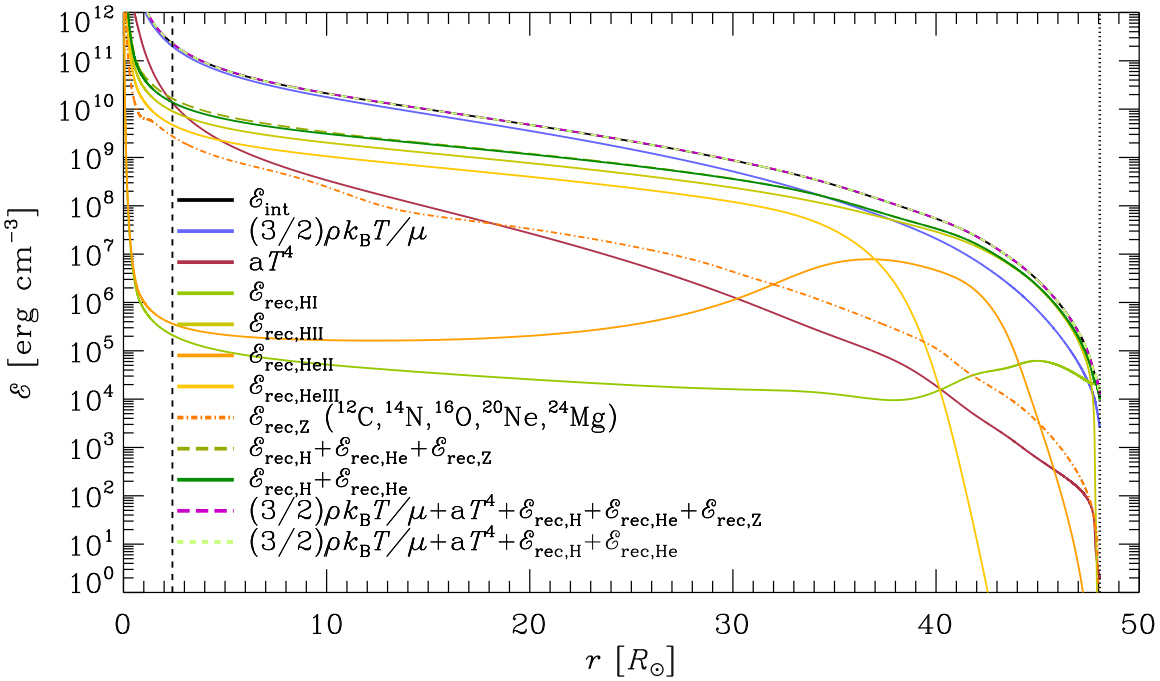

Figure 1. MESA r12778.

Table 1. List of runs

Run	Description	Physical scenario
A	MESA EoS, excluding radiation energy	Immediate local thermalization of released recombination energy
B	$\gamma = 5/3$ ideal gas EoS	Constant uniform composition (no accounting for ionization and recombination)
C	MESA EoS, excluding radiation and recombination energy	Immediate radiative loss of released recombination energy

4.3.2 *Hydrogen and Helium*

- Mention Fig. 2 and Fig. 3, 2nd row (temperature), 3rd row (ionization state) and 4th row (tracer)
- Explain how recombination is underestimated at late times (re-ionization of some of He)
- Mention Fig. 8 (energy released/absorbed by ionic transitions of He)
- Mention Fig. 9 (total released/absorbed energy from all ionic transitions)
- Explain how recombination is underestimated (e.g. H recom en curve peaks)
- This is confirmed by last time plotted in fig showing morphology, where, e.g., re-ionization of helium is apparent.

5 DISCUSSION

5.1 Nullifying the influence of the ambient medium

- Explain how ambient medium params are chosen
- Explain tradeoff between maximizing stability and minimizing role of ambient
- Contrast simulations setups and results (e.g. separation curve) with other works (Ohlmann, Prust+Chang)
- Plan for future work

6 CONCLUSIONS

Summary of what was done
Summary of main findings:

- The orbital separation continues to decrease at the end of the simulation, and the mutual energy of the core particles reduces at an almost constant rate. When combined with the energy formalism, this suggests a CE timescale of 1–10 yr (for $\alpha_{\rm CE} \sim 0.5$–0.1), assuming that this rate stays constant.
- We verified that released recombination energy helps to unbind the envelope, finding a 10–20 per cent increase compared to the ideal gas simulation during the first half, when the energy transfer from the ambient medium is still negligible.
- However, release of recombination energy also expands the envelope, reducing the drag force, and leading to a smaller release of orbital energy relative to the ideal gas simulation. Thus, we find a *stabilizing* effect which limits the gain in unbound mass caused by the release of recombination energy.
- The run with the tabular EOS with internal energy replaced by thermal energy gives similar, though not identical, results to the ideal gas run. This helps to confirm soundness of the methods but suggests other effects in the tabular EOS play a small role (and apparently also promote unbinding).
- Tracking gas that is *initially* comprised of a given ionization species, and comparing it to the present ionization species of that

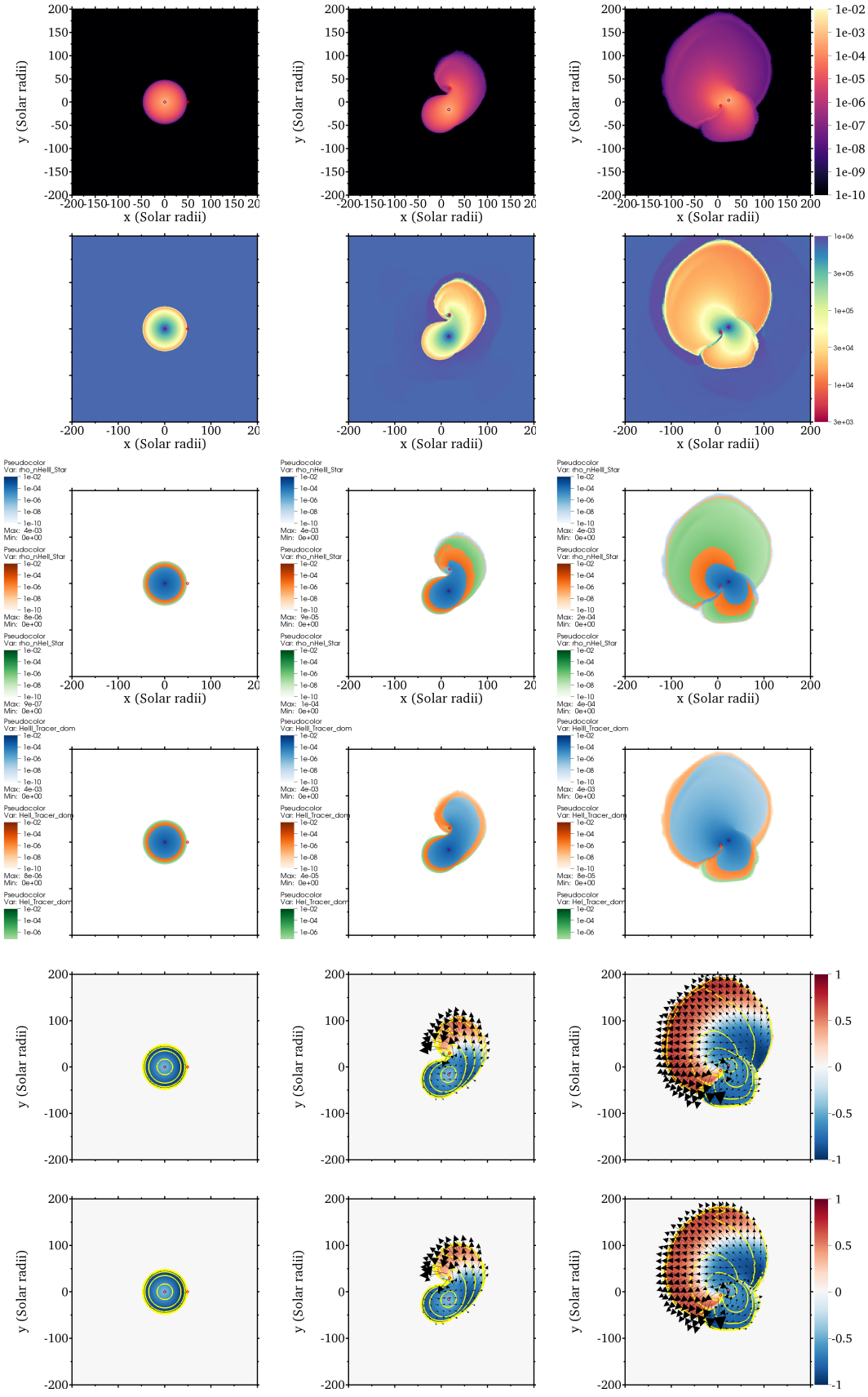

Figure 2. Columns show t = 0, 5.8 and 11.6 d. Rows are: (1) Normalized binding energy density of star tracer gas for Run 282 (γ = 5/3 ideal gas), (2) Normalized binding energy density of star tracer gas for Run 277 (MESA EOS without radiation energy)), (3) Gas density at location where a given He tracer density is highest for Run 277, (4) Gas density at location where a given He ionization state is highest, (5) Gas temperature, (6) Gas density.

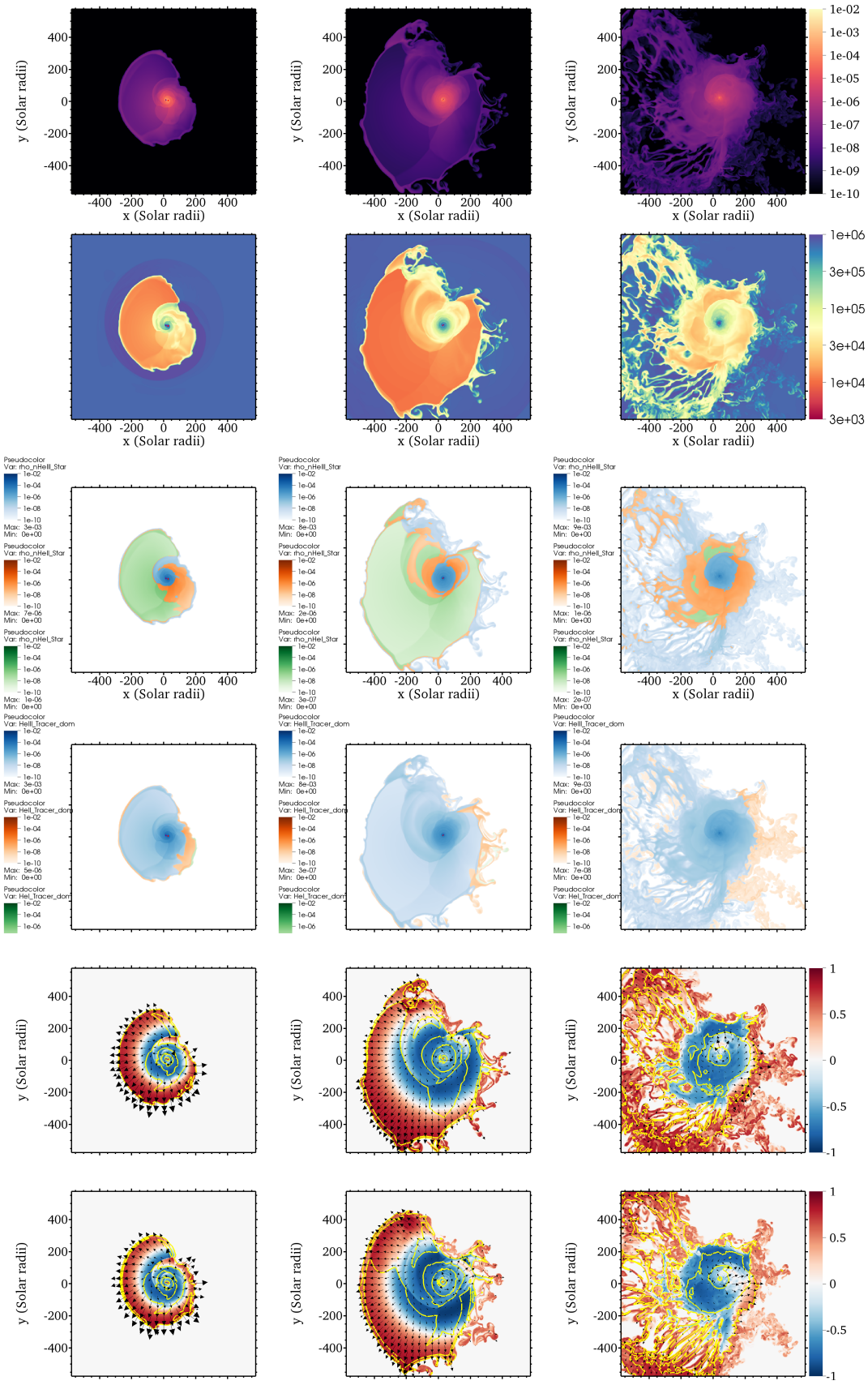

Figure 3. Continuation of Fig. 2 for times t = 23.1, 46.3 and 92.6 d.

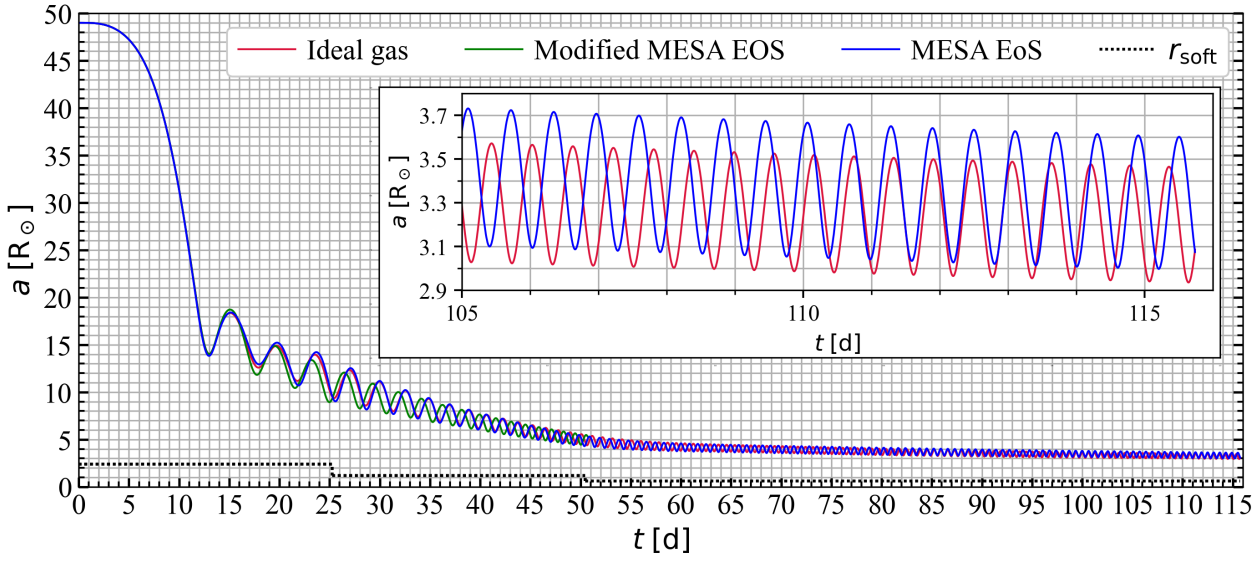

Figure 4.

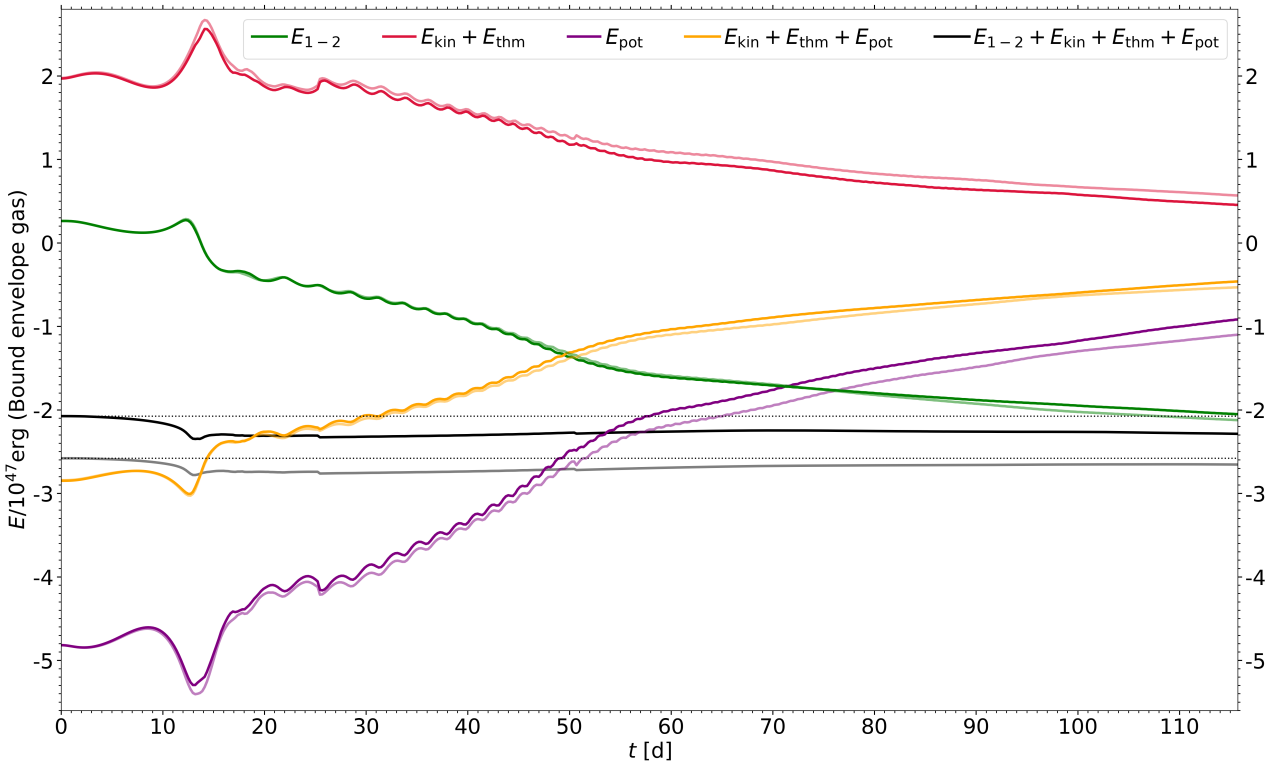

Figure 5. .

gas calculated using the Saha equation, is an effective way to track recombination and ionization in the simulation.

- For the first half of the simulation, recombination energy released by helium and hydrogen into bound envelope gas, predicted from this method, agrees well with that computed by differencing internal and thermal energy components of the gas. Thereafter, the latter method yields a higher value, suggesting that recombination of metals become important once the envelope expands enough. This is consistent with order of magnitude estimates [Luke comments: must check more carefully].

ACKNOWLEDGEMENTS

The authors thank Paul Ricker and Thomas Reichardt for discussions. This work used the computational and visualization resources in the Center for Integrated Research Computing (CIRC) at the University of Rochester and the computational resources of the Texas Advanced Computing Center (TACC) at The University of Texas at Austin, provided through allocation TG-AST120060 from the Extreme Science and Engineering Discovery Environment (XSEDE) (Towns et al. 2014), which is supported by National Science Found-

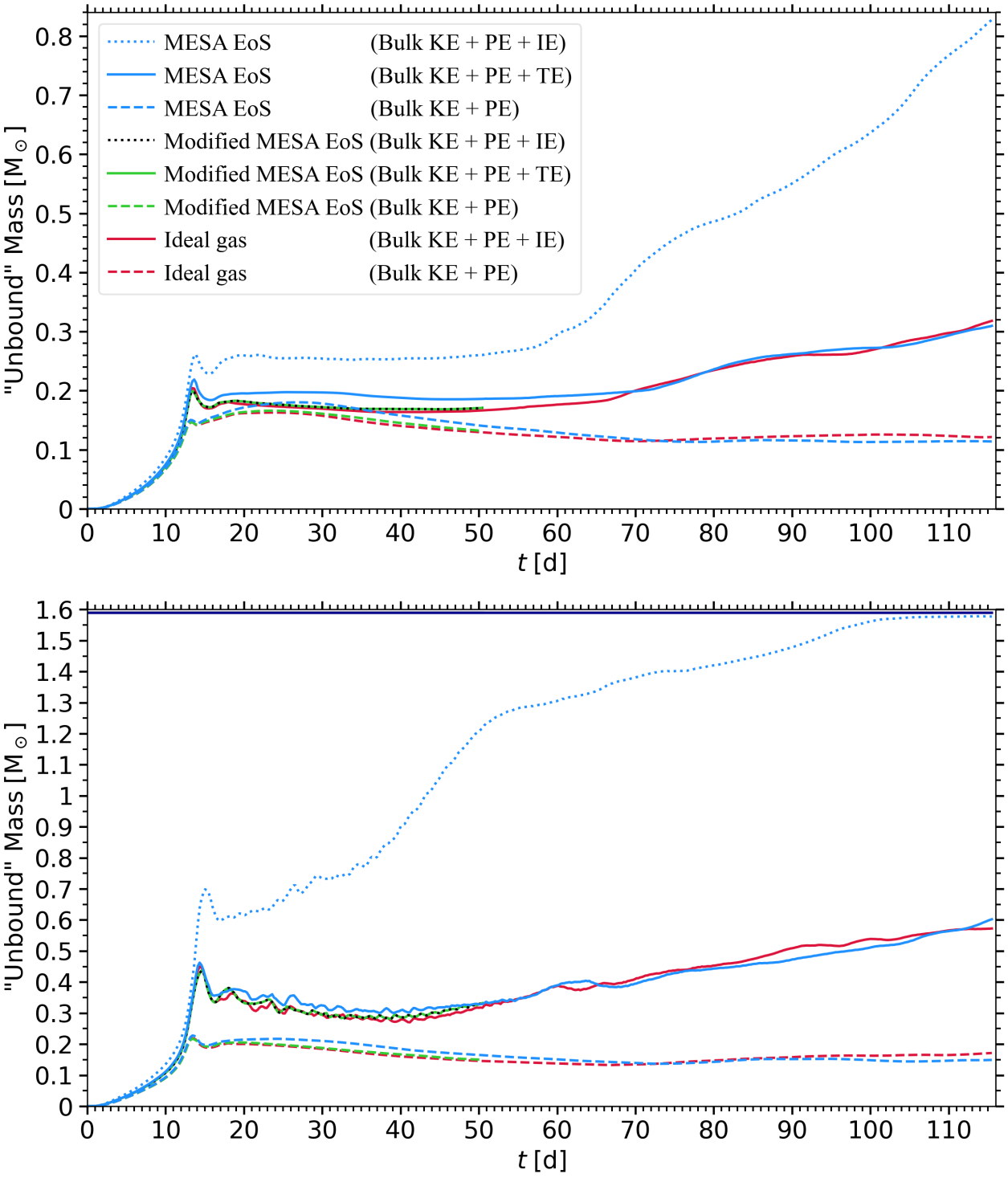

Figure 6.

ation grant number ACI-1548562. [Luke comments: Add Jason's XSEDE allocation info and TACC Frontera allocation info.] Financial support for this project was provided by the Department of Energy grants DE-SC0020432 and DE-SC0020434, the National Science Foundation grant AST-1813298 and the National Aeronautics and Space Administration grant 80NSSC20K0622.

References

Carroll-Nellenback J. J., Shroyer B., Frank A., Ding C., 2013, Journal of Computational Physics, 236, 461

Chamandy L., et al., 2018, MNRAS, 480, 1898

Chamandy L., Tu Y., Blackman E. G., Carroll-Nellenback J., Frank A., Liu B., Nordhaus J., 2019a, MNRAS, 486, 1070

Chamandy L., Blackman E. G., Frank A., Carroll-Nellenback J., Zou Y., Tu Y., 2019b, MNRAS, 490, 3727

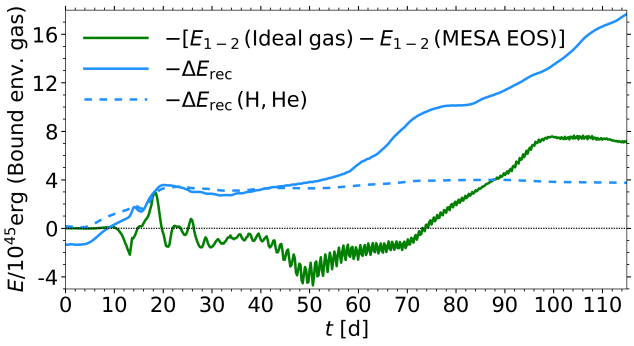

Figure 7.

Chamandy L., Blackman E. G., Frank A., Carroll-Nellenback J., Tu Y., 2020, MNRAS, 495, 4028
Cunningham A. J., Frank A., Varnière P., Mitran S., Jones T. W., 2009, ApJS, 182, 519
Grichener A., Sabach E., Soker N., 2018, MNRAS, 478, 1818
Ivanova N., 2018, ApJ, 858, L24
Ivanova N., Justham S., Avendano Nandez J. L., Lombardi J. C., 2013, Science, 339, 433
Ivanova N., Justham S., Ricker P., 2020, Common Envelope Evolution, doi:10.1088/2514-3433/abb6f0.
Lau M. Y. M., Hirai R., González-Bolívar M., Price D. J., De Marco O., Mandel I., 2022, MNRAS,
Ohlmann S. T., 2016, PhD thesis, -
Ohlmann S. T., Röpke F. K., Pakmor R., Springel V., 2017, A&A, 599, A5
Paczynski B., 1976, in Eggleton P., Mitton S., Whelan J., eds, IAU Symposium Vol. 73, Structure and Evolution of Close Binary Systems. p. 75
Paxton B., Bildsten L., Dotter A., Herwig F., Lesaffre P., Timmes F., 2011, ApJS, 192, 3
Paxton B., et al., 2013, ApJS, 208, 4
Paxton B., et al., 2015, ApJS, 220, 15
Paxton B., et al., 2019, ApJS, 243, 10
Reichardt T. A., De Marco O., Iaconi R., Chamandy L., Price D. J., 2020, MNRAS,
Sabach E., Hillel S., Schreier R., Soker N., 2017, MNRAS, 472, 4361
Sand C., Ohlmann S. T., Schneider F. R. N., Pakmor R., Röpke F. K., 2020, A&A, 644, A60
Soker N., Harpaz A., 2003, MNRAS, 343, 456
Soker N., Grichener A., Sabach E., 2018, preprint, (arXiv:1805.08543)
Towns J., Cockerill T., Dahan M., Foster I., 2014, Computing in Science and Engineering, 16, 62

APPENDIX A: EFFECTS OF VARYING THE NUMERICAL PARAMETERS

A1 Resolution

- 1. Figure showing separation, comparing different resolutions (low, standard, high)
- 2. Figure showing unbound mass (for at least one definition of unbound), comparing different resolutions (low, standard, high)

A2 Ambient density

- 1. Figure showing separation, comparing different ambient densities (runs 277 and 271)
- 2. Figure showing unbound mass, comparing different ambient densities (runs 277 and 271)

A3 Energy and angular momentum conservation

- 1. Figure showing energy conservation (for all the runs)
- 2. Figure showing angular momentum conservation (for all the runs)

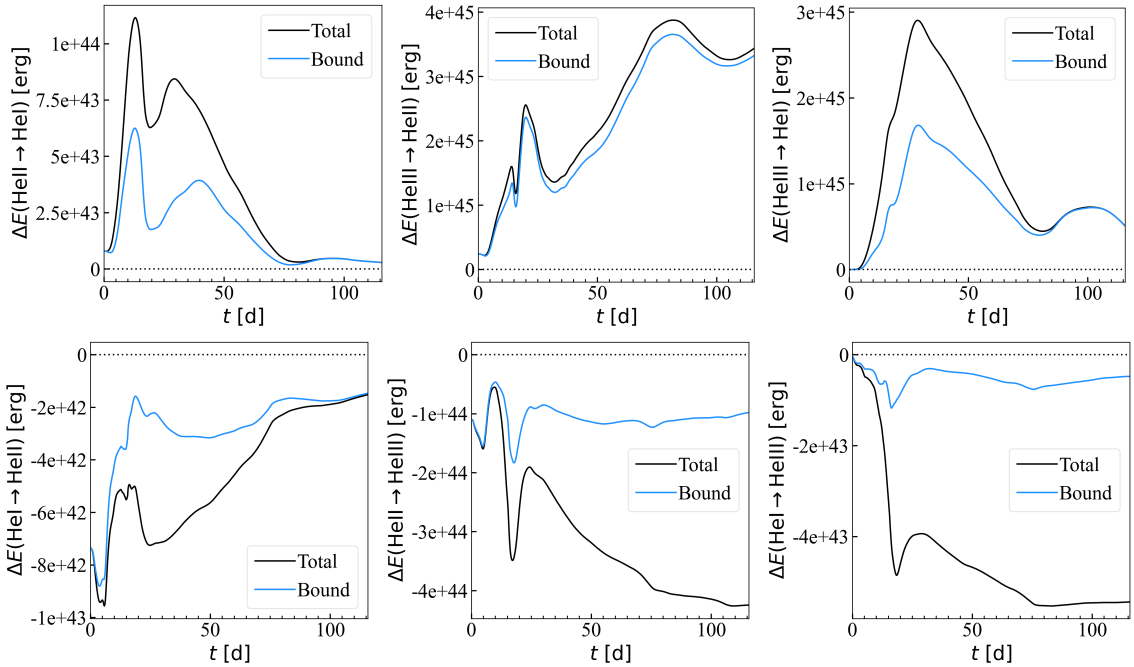

Figure 8. Energy released by each ionic transition of helium. Recombination results in positive values whereas ionization results in negative values. The red (blue) curve shows the amount of energy that has been released by gas that is unbound (bound) at time t.

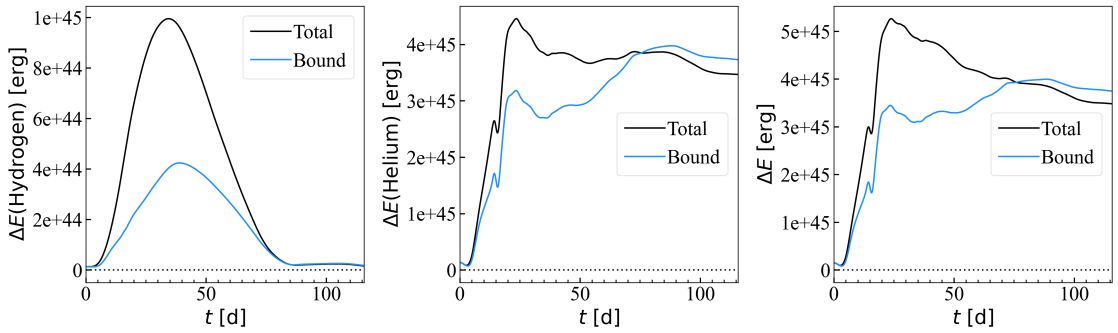

Figure 9. Release of energy from recombination (left column) and ionization (middle column) of H (top row), He (middle row), and their combination (bottom row). The net energy release is plotted in the right column. Note that the ambient gas is excluded (as it should be). The red (blue) curve shows the amount of energy that has been released by gas that is unbound (bound) at time t.